Numerical modeling of Radio jets from YSOs

Thermal + non-thermal emission from jets

HH80-81

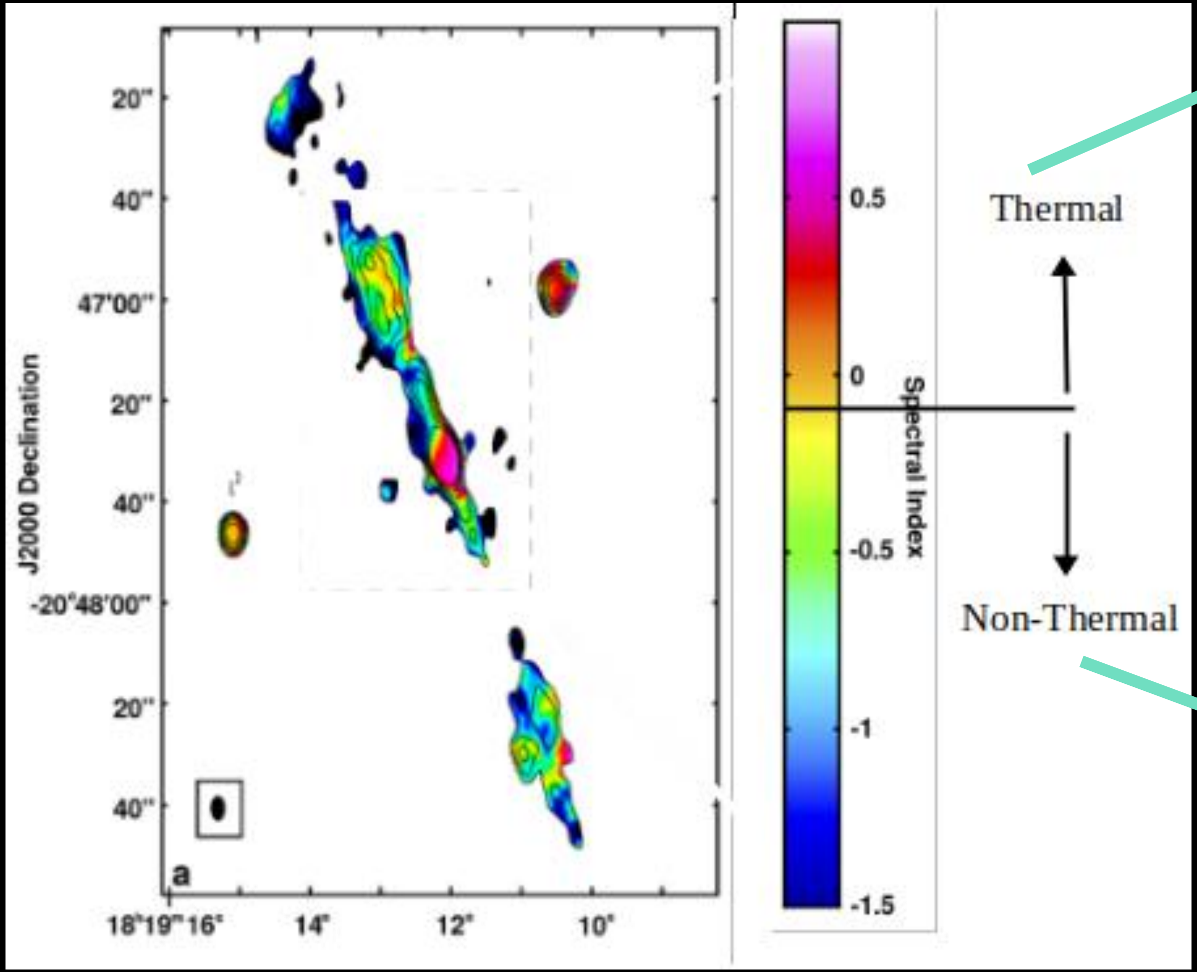

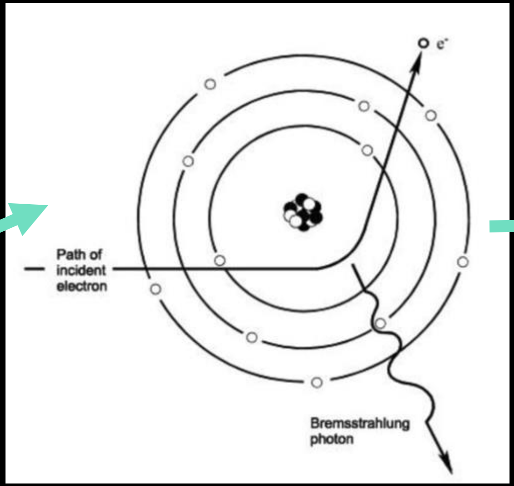

Credit: Ignacio Aviles

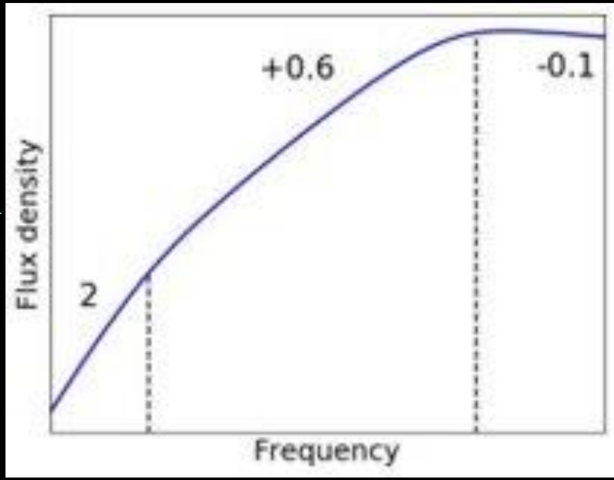

Free-free emission spectrum

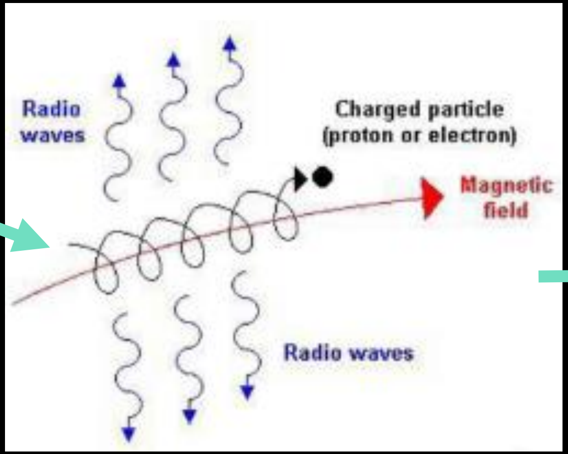

Credit: http://nrumiano.free.fr

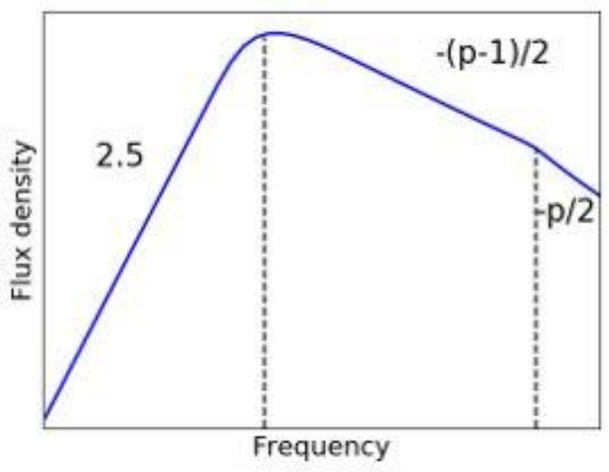

Synchrotron emission spectrum

Motivation

- Develop a model to characterize the radio spectra of protostellar jets: Thermal + non-thermal emission

- Reynolds (1986) model: $S_\nu \propto \nu^\alpha$; $\alpha = +0.6$ for a spherical, isothermal, constant velocity thermal jet.
- Reynolds (1986) model limitations:
    - Only free-free emission is considered
    - Assumes that the jet is optically thick at the base and thin at farther radial distances.
    - Applicable only to narrow collimated jets

- Advantages of our model:
    - Free-free + synchrotron mechanisms
    - Incorporates generalized geometry (16–20%)
    - Incorporates intermediate optical depth (8 – 12%)
    - Lateral variation of ionization fraction

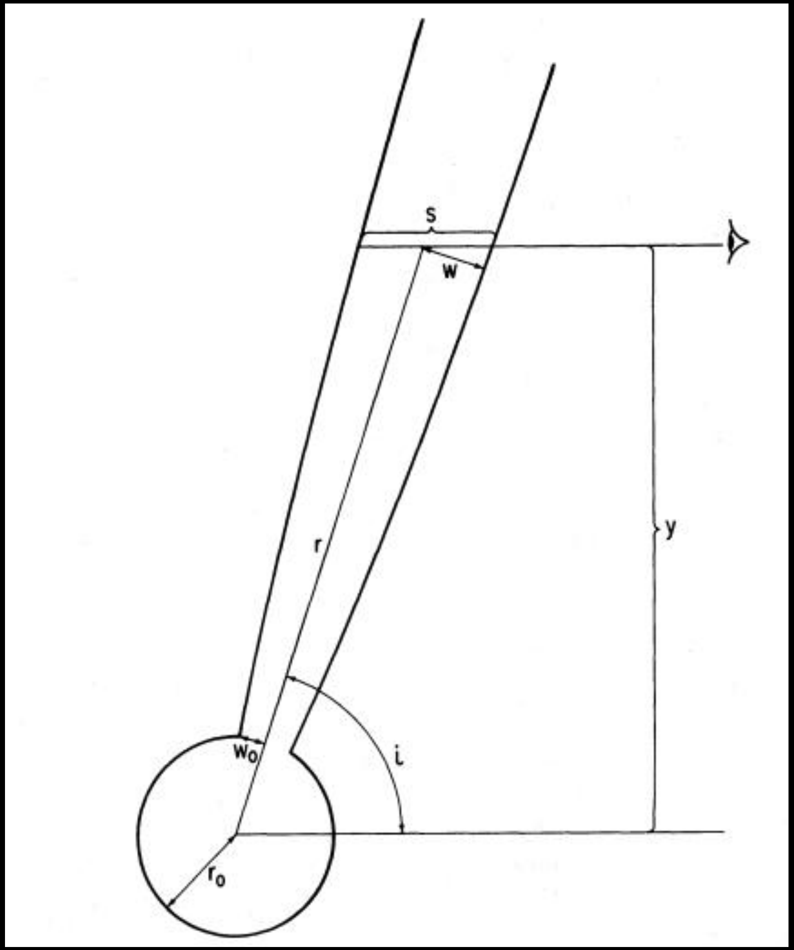

Reynolds (1986)

Model description

Model : Brief discussion

Jet geometry : Inner thermal jet + thin shocked shell

$$
\begin{aligned}
y &= r \sin i \\
\omega &= \omega_0 \left(\frac{r}{r_0} \right)^{\epsilon} = \omega_0 \left(\frac{y}{y_0} \right)^{\epsilon}
\end{aligned}
$$

- **Radial Variation:**
  - **ω, θ, x, n**
- **Lateral Variation:**
  - **x**

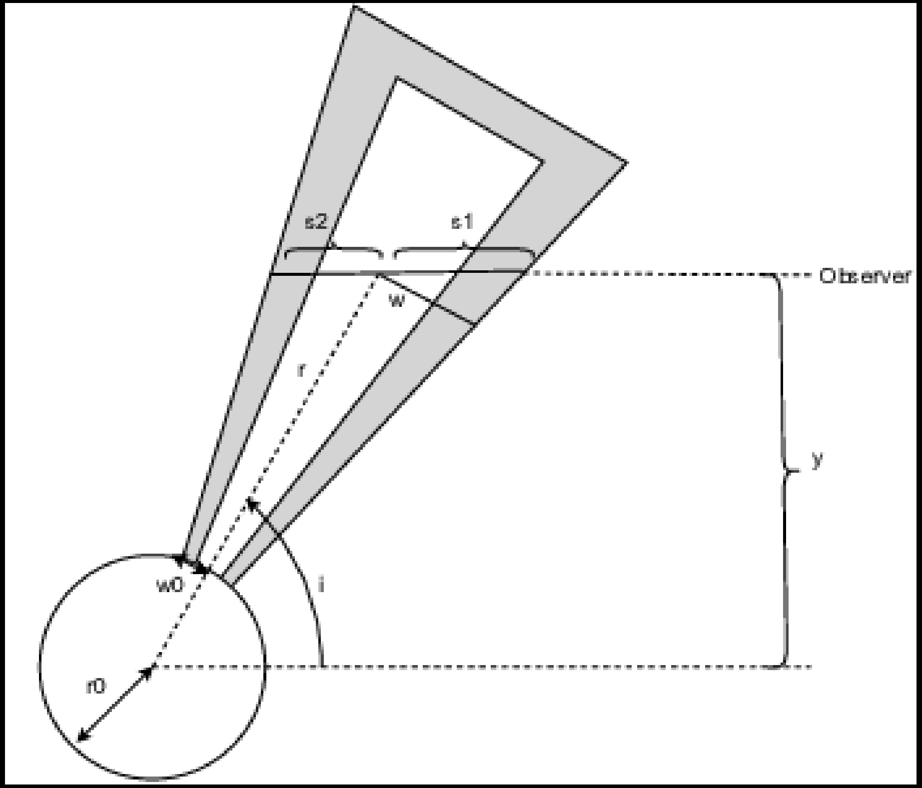

Side view

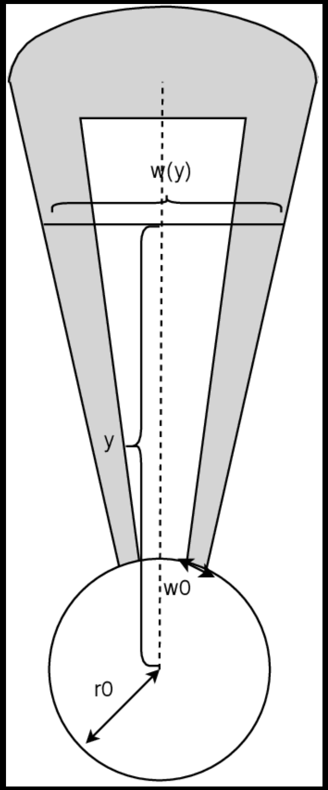

Front view

The shaded region represents the thin shocked material

ω: jet half-width, θ: opening angle, x: ionization fraction, n: number density

Model: Lateral variation in ionization fraction

Onion-like/nested velocity structure

- High velocity gas collimated into a small opening angle towards the axis of the jet/outflow
- Less collimated low velocity gas with a wide opening angle
- Assuming that ionization is a result of internal/external shocks, the strength of which depends on velocity
- Higher velocity regions creates stronger shocks resulting in higher ionization fraction

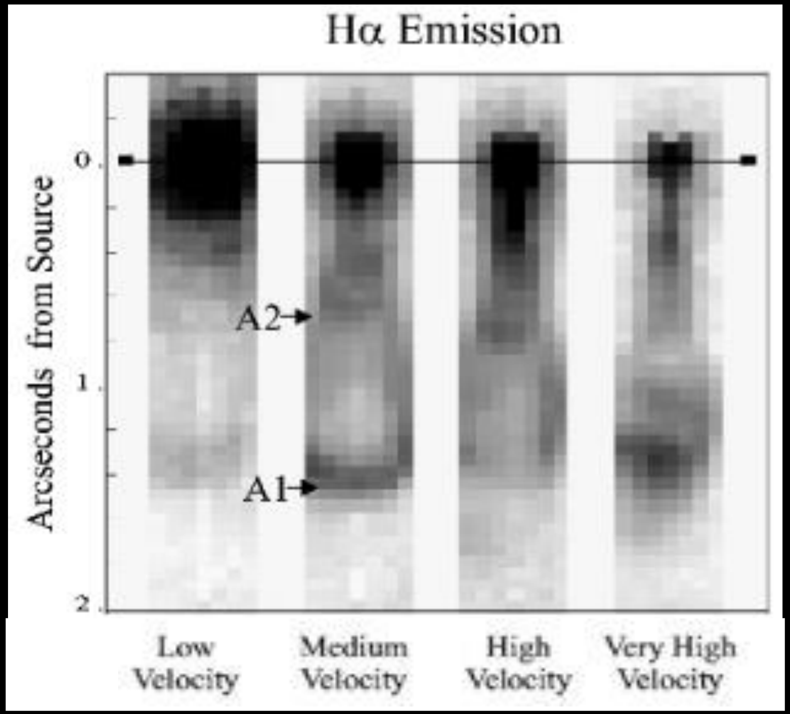

DG Tau jet, Bacciotti et al. 2002

Model: Lateral variation in ionization fraction

Onion-like/nested velocity structure

- High velocity gas collimated into a small opening angle towards the axis of the jet/outflow
- Less collimated low velocity gas with a wide opening angle
- Assuming that ionization is a result of internal/external shocks, the strength of which depends on velocity
- Higher velocity regions creates stronger shocks resulting in higher ionization fraction

$$x(s) = x_a(y')\left[\frac{w(y')}{w(y') - w'(y')}\right]^{q'_x}$$

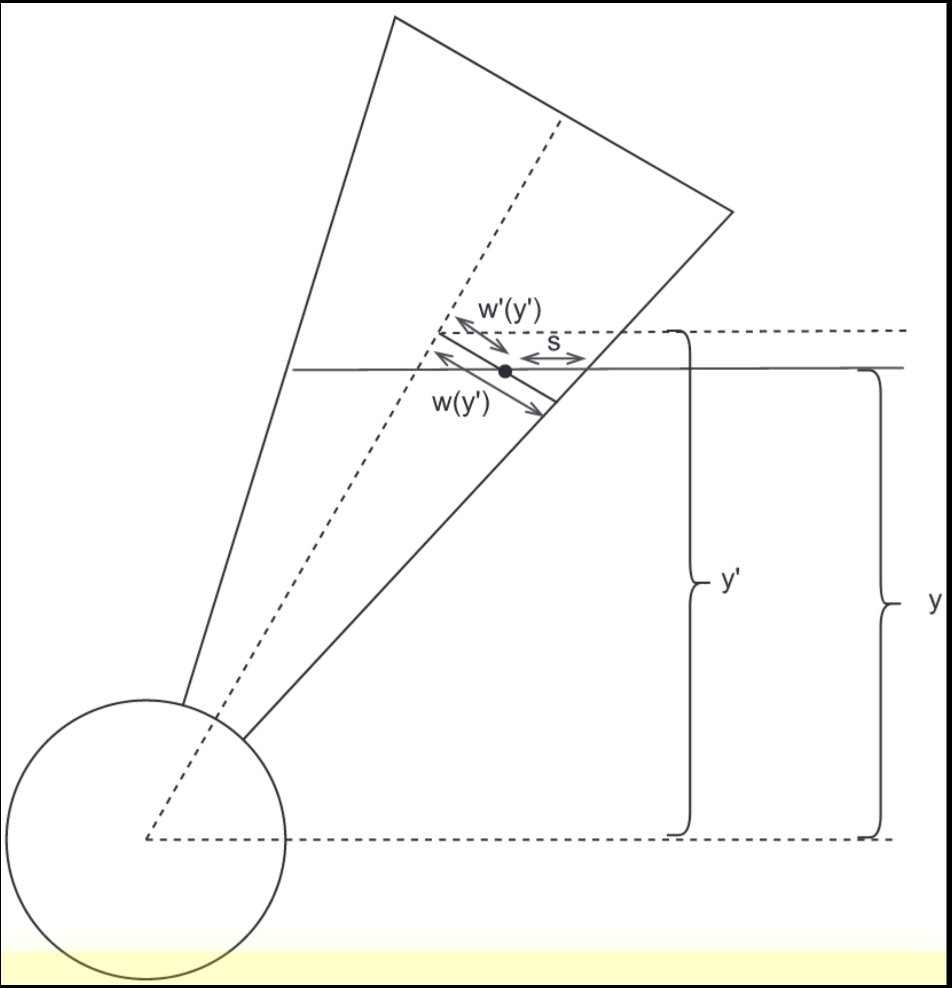

Model : LOS flux density

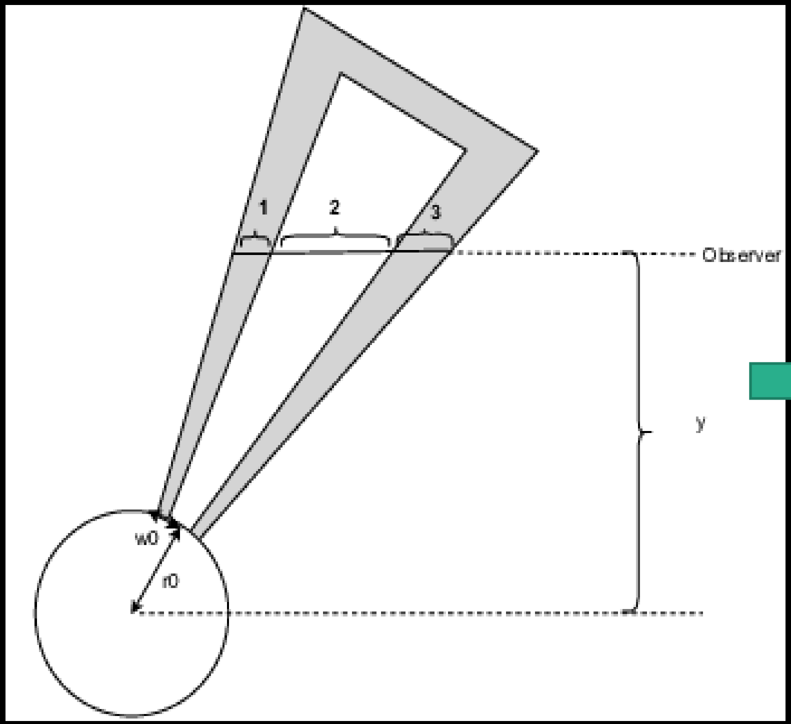

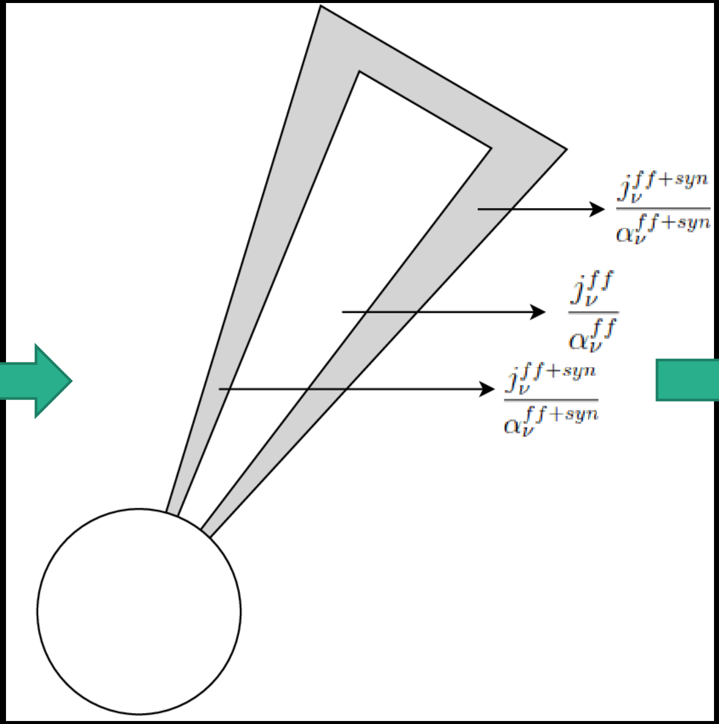

$$C_{1_\nu} n^{ff}(s)^2 + C_{2_\nu} n^{syn}(s)$$

$$I_{\nu_1}^{ff+syn} = \int_0^{\tau_{\nu_1}^{ff+syn}} \frac{j_{\nu_1}^{ff+syn}(s)}{\alpha_{\nu_1}^{ff+syn}(s)} e^{-(\tau_{\nu_1}^{ff+syn} - \tau(s))} d\tau$$

$$I_{\nu_2}^{ff+syn} = \frac{j_{\nu_2}^{ff}}{\alpha_{\nu_2}^{ff}} (1 - e^{-\tau_{\nu_2}^{ff}})$$

$$\propto (n^{ff})^2$$

$$I_{\nu_3}^{ff+syn} = \int_0^{\tau_{\nu_3}^{ff+syn}} \frac{j_{\nu_3}^{ff+syn}(s)}{\alpha_{\nu_3}^{ff+syn}(s)} e^{-(\tau_{\nu_3}^{ff+syn} - \tau(s))} d\tau$$

Region 1 & 3: Free-Free + Synchrotron
Region 2 : purely Free-Free

$$I_\nu(y) = I_{\nu_1}^{ff+syn} \, e^{-(\tau_{\nu_2}^{ff} + \tau_{\nu_3}^{ff+syn})} + I_{\nu_2}^{ff+syn} \, e^{-\tau_{\nu_3}^{ff+syn}} + I_{\nu_3}^{ff+syn}$$

Two-fold application of the model

- YSO jets have been seen to appear as chains of well-defined knots/lobes powered by the central object, instead of being a continuous outflow
- Knots have been identified in a wide range of bands from radio to X-rays

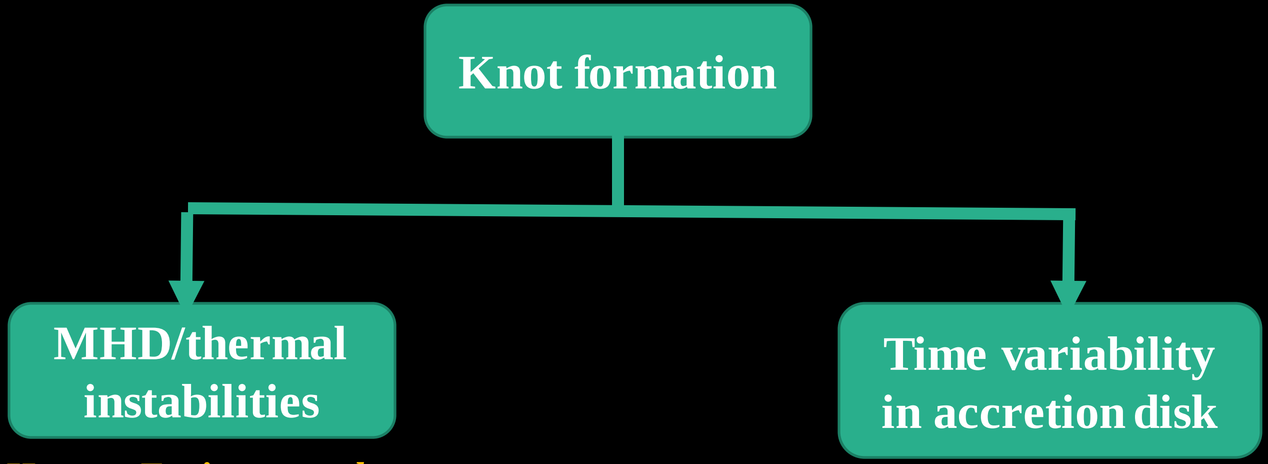

Huarte-Espinosa et al. 2012; Lebedev et al. 2005

Bonito et al. 2010

[SII] HST

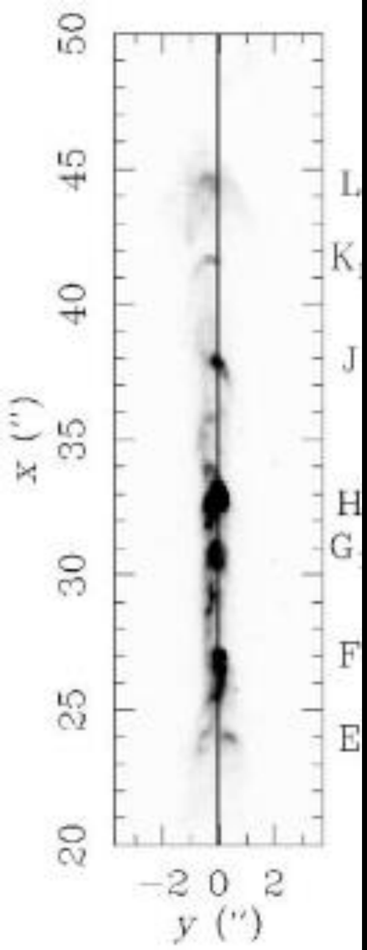

HH 111, Raga et al. 2002

2cm VLA

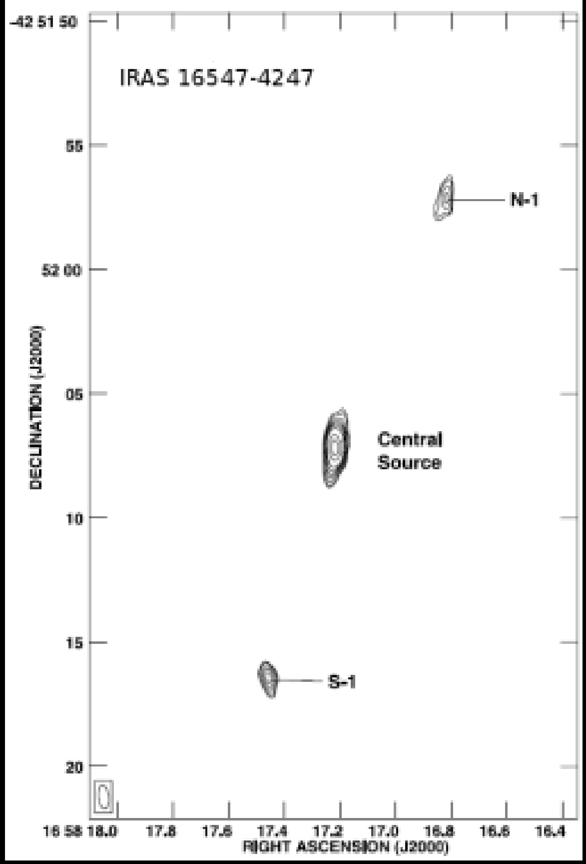

Rodriguez et al. 2005

Two-fold application of the model

- Observations indicate presence of non-thermal emission from knots/lobes of few YSO jets, while in most cases the emission can be explained due to thermal free-free mechanism.

Spectral indices

Inner thermal jet ← $+0.2 \pm 0.01$

Outer knots/lobes ← -0.26 ± 0.01, -0.63 ± 0.19

(Vig et al. 2018)

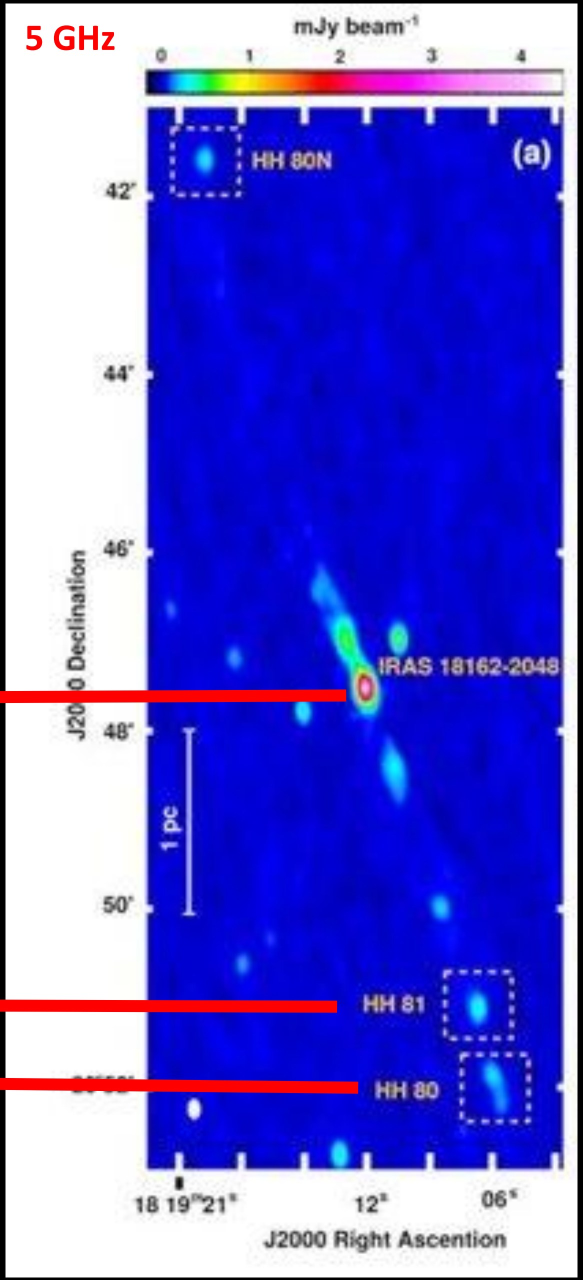

HH80-81 jet, Carrasco-Gonzalez 2010

Results

Effect of jet parameters on free-free emission

- Case of a fully thermal jet
- Located close to the central YSO (r_0 = 10-50 au)
  - r_0: Jet injection radius
  - n_0: Jet number density at r_0
  - q_n: Power-law index of n profile

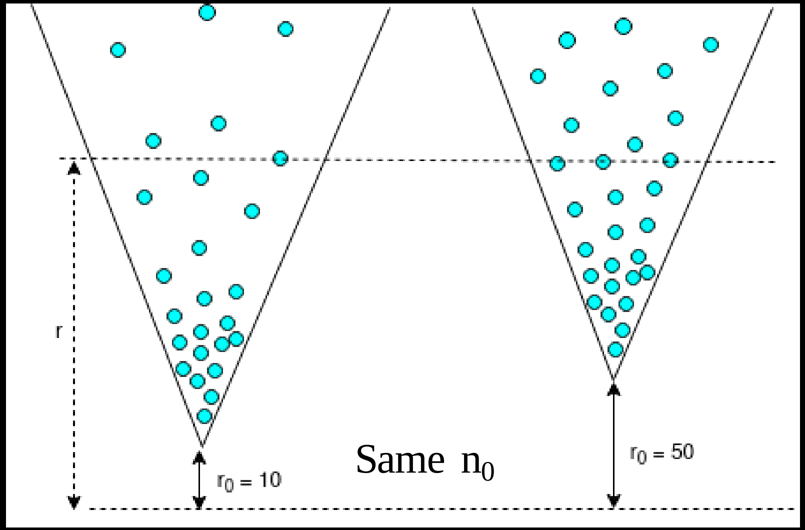

$$n = n_0 \left(\frac{r}{r_0}\right)^{q_n} = n_0 \left(\frac{y}{y_0}\right)^{q_n}$$

n_0, q_n, r_0

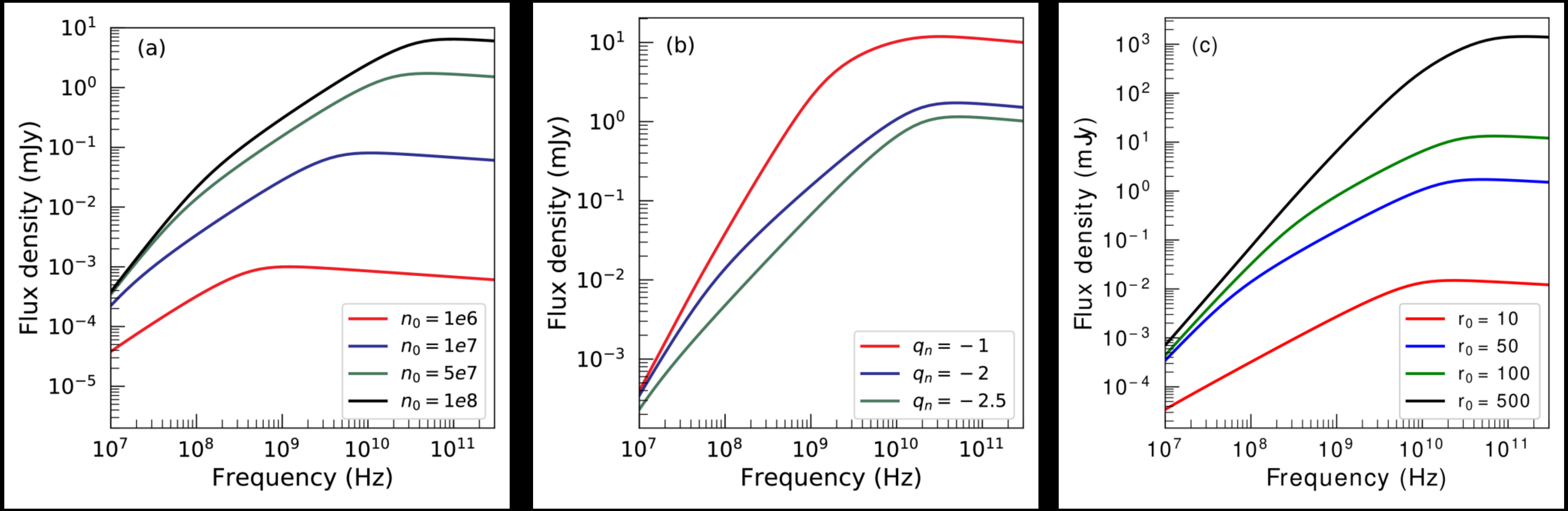

Effect of jet parameters on free-free emission

r_0, r_{LOSmax}

Variable parameter	Value	Turnover frequencies (GHz)	Spectral indices
n_0	10^6	0.76	0.80; −0.09
	10^7	0.04; 6.87	1.30; 0.83; −0.09
(cm^{-3})	5×10^7	0.18; 31.17	1.57; 0.83; −0.06
	10^8	0.35; 60.59	1.65; 0.84; −0.04
q_n	−1	1.67; 32.70	1.86; 0.36; −0.08
	−2	0.18; 31.17	1.57; 0.83; −0.06
	−2.5	0.03; 30.58	1.43; 1.04; −0.06
r_0	10	14.92	0.88; −0.07
	50	0.18; 31.17	1.57; 0.83; −0.06
(au)	100	0.86; 45.52	1.72; 0.76; −0.06
	500	101.35	1.71; −0.01

n_0,

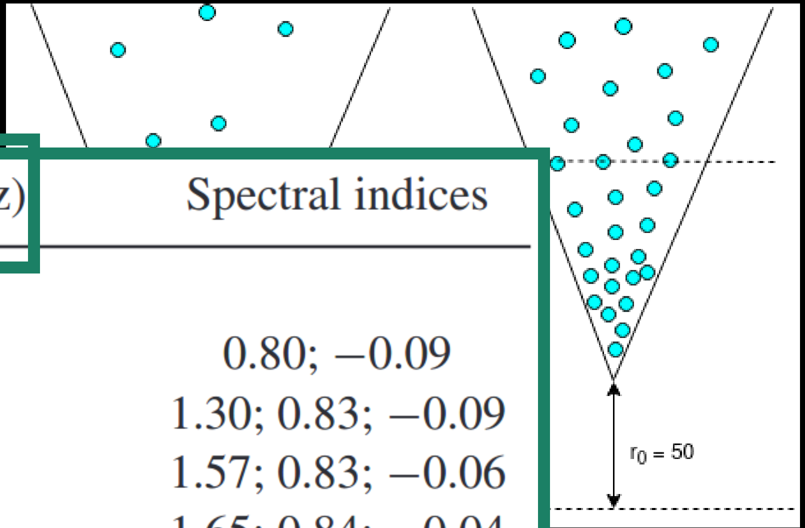

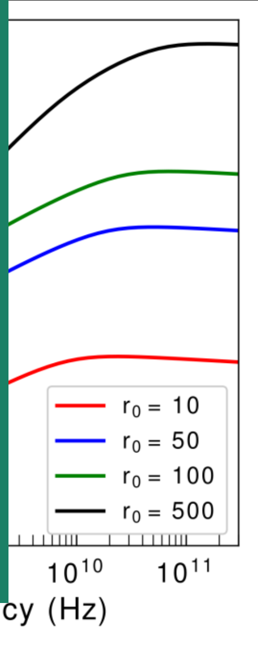

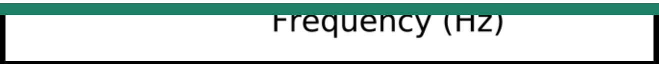

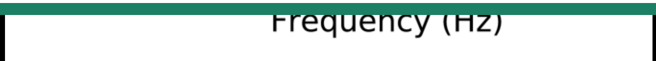

Effect of jet parameters on fre
emission

r_0, r_{LOSmax}

Variable parameter	Value	Turnover frequencies (GHz)	S
n_0	10^6	0.76	0.80; −0.09
	10^7	0.04; 6.87	1.30; 0.83; −0.09
(cm^{-3})	5×10^7	0.18; 31.17	1.57; 0.83; −0.06
	10^8	0.35; 60.59	1.65; 0.84; −0.04
q_n	−1	1.67; 32.70	1.86; 0.36; −0.08
	−2	0.18; 31.17	1.57; 0.83; −0.06
	−2.5	0.03; 30.58	1.43; 1.04; −0.06
r_0	10	14.92	0.88; −0.07
	50	0.18; 31.17	1.57; 0.83; −0.06
(au)	100	0.86; 45.52	1.72; 0.76; −0.06
	500	101.35	1.71; −0.01

n_0,

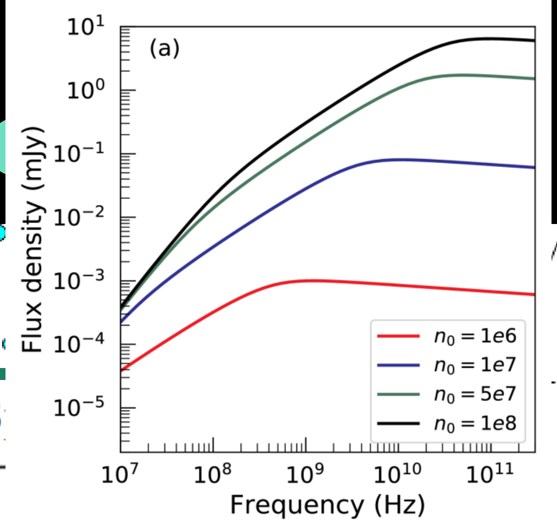

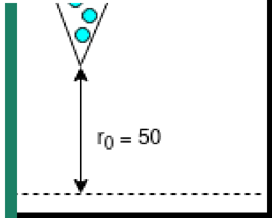

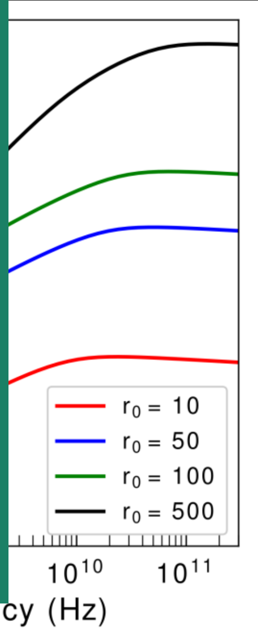

Frequency (Hz)

Frequency (Hz)

Effect of jet parameters on free-free emission

r_0, r_{LOSmax}

Variable parameter	Value	Turnover frequencies (GHz)	Spectral indices
n_0 (cm^{-3})	10^6	0.76	0.80; −0.09
	10^7	0.04; 6.87	1.30; 0.83; −0.09
	5×10^7	0.18; 31.17	1.57; 0.83; −0.06
	10^8	0.35; 60.59	1.65; 0.84; −0.04
q_n	−1	1.67; 32.70	1.86; 0.36; −0.08
	−2	0.18; 31.17	1.57; 0.83; −0.06
	−2.5	0.03; 30.58	1.43; 1.04; −0.06
r_0 (au)	10	14.92	0.88; −0.07
	50	0.18; 31.17	1.57; 0.83; −0.06
	100	0.86; 45.52	1.72; 0.76; −0.06
	500	101.35	1.71; −0.01

n_0,

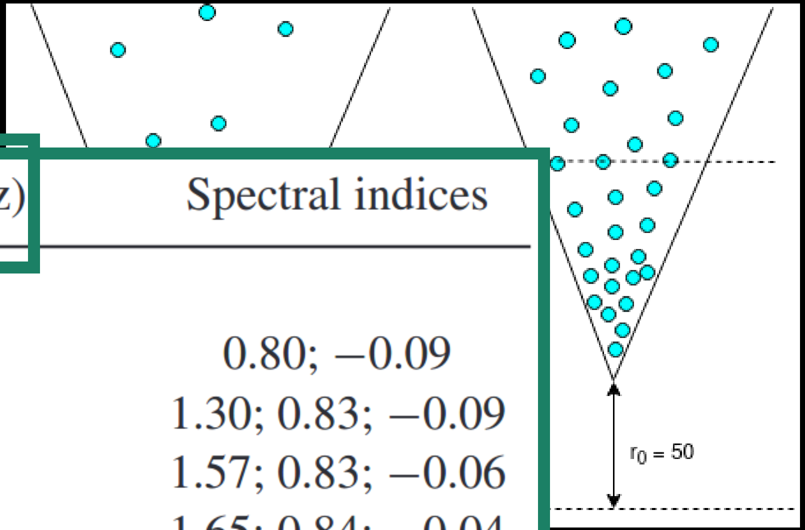

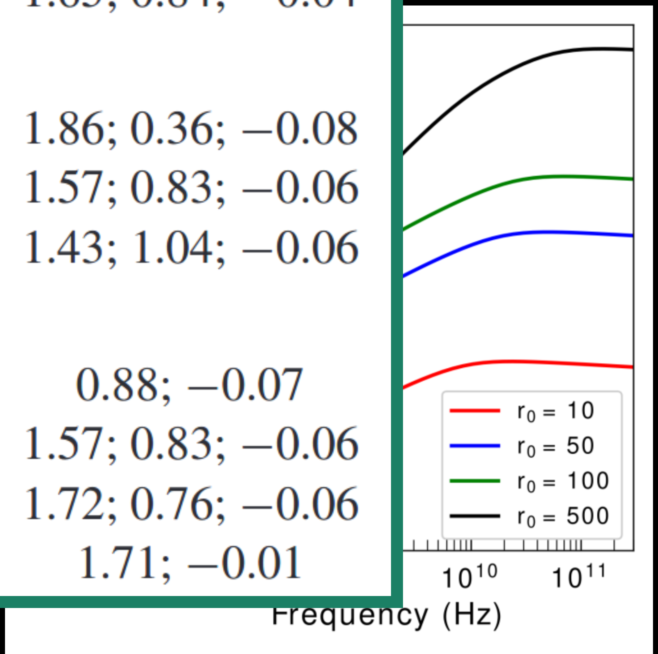

Frequency (Hz)

Frequency (Hz)

Effect of jet parameters on free-free emission

r_0, r_{LOSmax}

n_0,

Variable parameter	Value	Turnover frequencies (GHz)	Spectral indices
n_0	10^6	0.76	0.80; −0.09
	10^7	0.04; 6.87	1.30; 0.83; −0.09
(cm^{-3})	5×10^7	0.18; 31.17	1.57; 0.83; −0.06
	10^8	0.35; 60.59	1.65; 0.84; −0.04
q_n	−1	1.67; 32.70	1.86; 0.36; −0.08
	−2	0.18; 31.17	1.57; 0.83; −0.06
	−2.5	0.03; 30.58	1.43; 1.04; −0.06
r_0	10	14.92	0.88; −0.07
	50	0.18; 31.17	1.57; 0.83; −0.06
(au)	100	0.86; 45.52	1.72; 0.76; −0.06
	500	101.35	1.71; −0.01

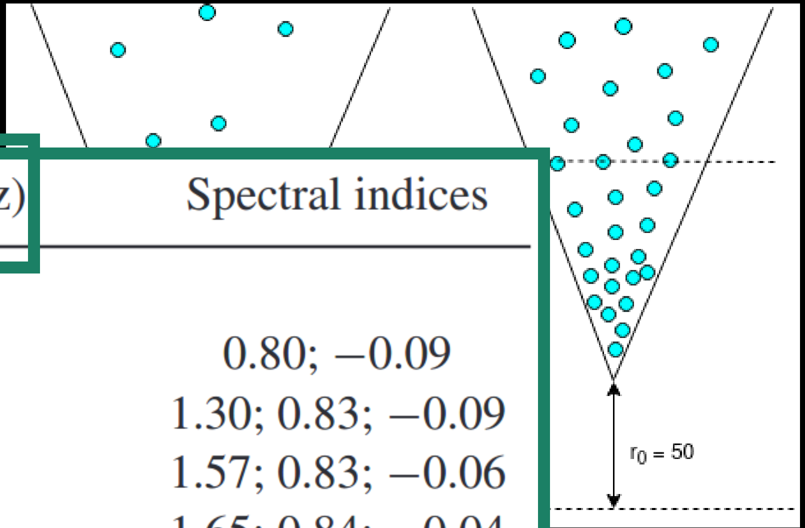

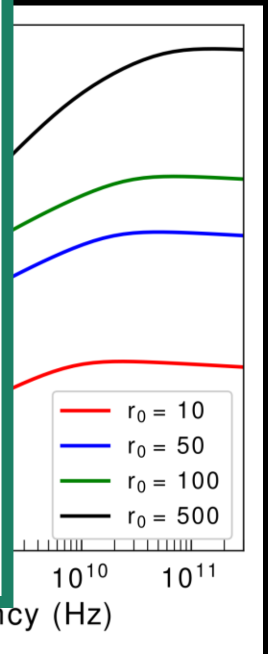

Frequency (Hz)

Frequency (Hz)

Effect of jet parameters on Synchrotron emission

- Jet with both thermal and non-thermal emission
- Located farther from the YSO (r0 = 3000 au)
  - B_0: Magnetic field strength at r_0
  - $\delta\theta$: Angular thickness of shocked shell
  - p: Power-law index of number density distribution of non-thermal electrons in energy space

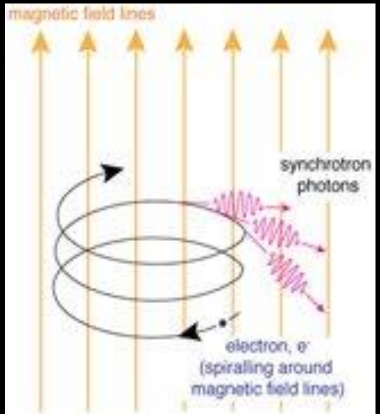

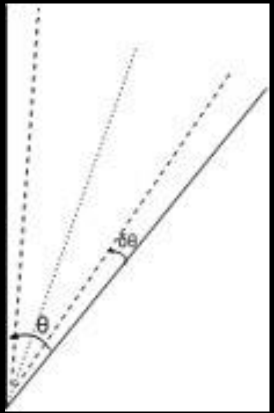

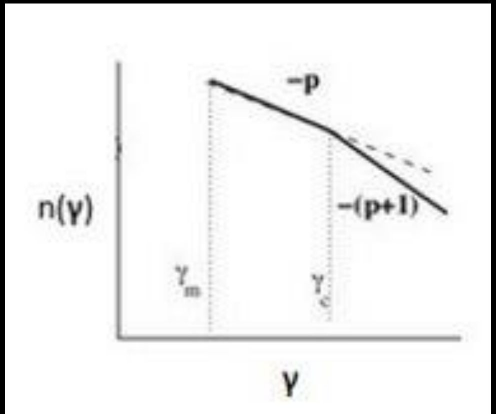

$B_{0,}\delta\theta$, p

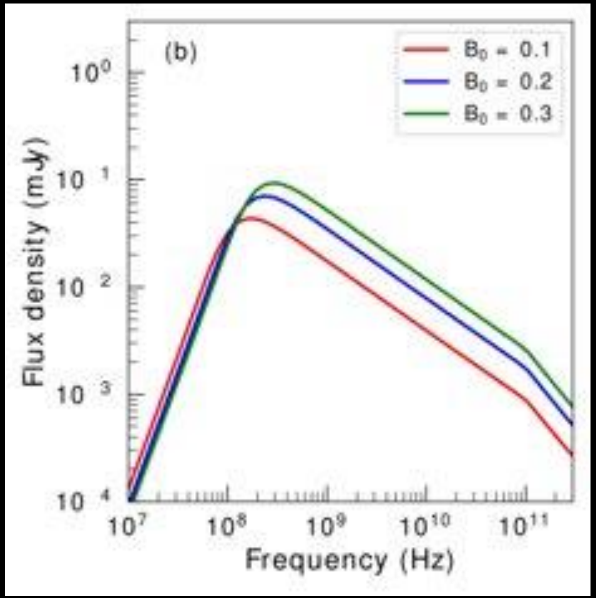

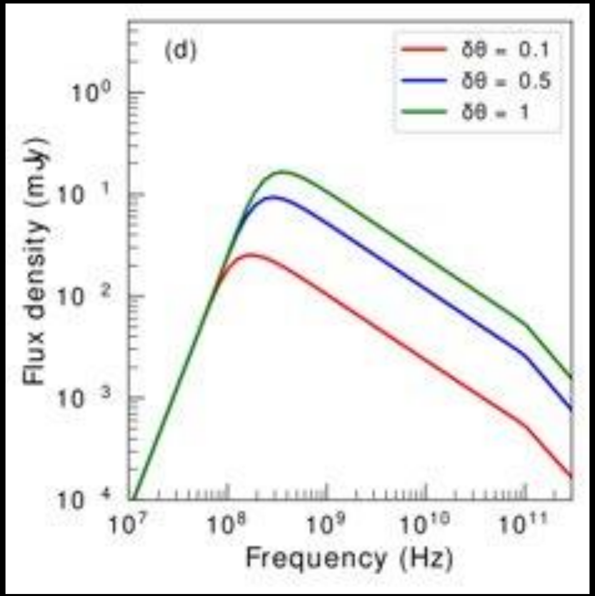

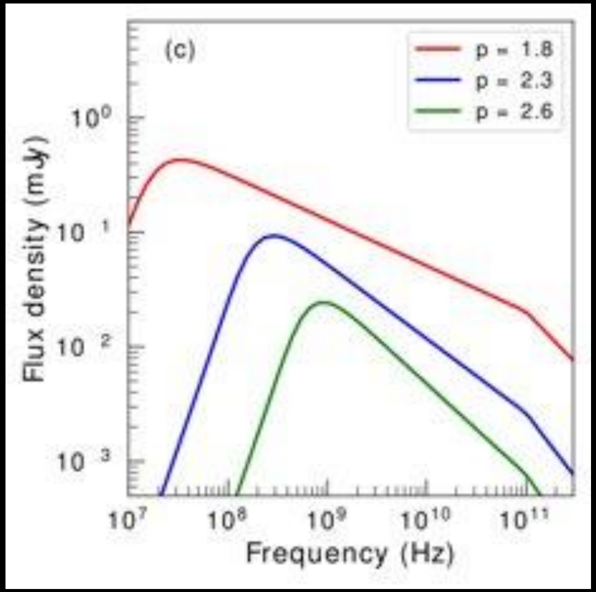

Effect of jet parameters on Synchrotron emission

$\propto \tau_{ff+syn} = 1,\ \nu_c$ (Govoni F., Feretti L., 2004)

- Jet with both thermal and non-thermal emission

Variable parameter	Value	Turnover frequencies (GHz)	Spectral indices
B_0	0.1	0.17; 100	2.20; −0.64; −1.10
	0.2	0.24; 100	2.20; −0.64; −1.1
(mG)	0.3	0.29; 100	2.31; −0.63; −1.13
p	1.8	0.03; 100	1.18; −0.40; −0.90
	2.3	0.29; 100	2.31; −0.63; −1.13
	2.6	0.90; 100	2.39; −0.77; −1.23
$\delta\theta$	0.1	0.17; 100	2.19; −0.63; −1.06
	0.5	0.29; 100	2.31; −0.63; −1.13
(°)	1	0.37; 100	2.26; −0.64; −1.14

Effect of jet parameters on Synchrotron emission

$\propto \tau_{ff+syn} = 1,\ \nu_c$ (Govoni F., Feretti L., 2004)

- **Jet with both thermal and non-thermal emission**

Variable parameter	Value	Turnover frequencies (GHz)	Spectral indices
B_0	0.1	0.17; 100	2.20; −0.64; −1.10
	0.2	0.24; 100	2.20; −0.64; −1.1
(mG)	0.3	0.29; 100	2.31; −0.63; −1.13
p	1.8	0.03; 100	1.18; −0.40; −0.90
	2.3	0.29; 100	2.31; −0.63; −1.13
	2.6	0.90; 100	2.39; −0.77; −1.23
$\delta\theta$	0.1	0.17; 100	2.19; −0.63; −1.06
	0.5	0.29; 100	2.31; −0.63; −1.13
(°)	1	0.37; 100	2.26; −0.64; −1.14

$\tau \propto B_0, p, \delta\theta$

Frequency (Hz)

Frequency (Hz)

Frequency (Hz)

Flux variation across jet length

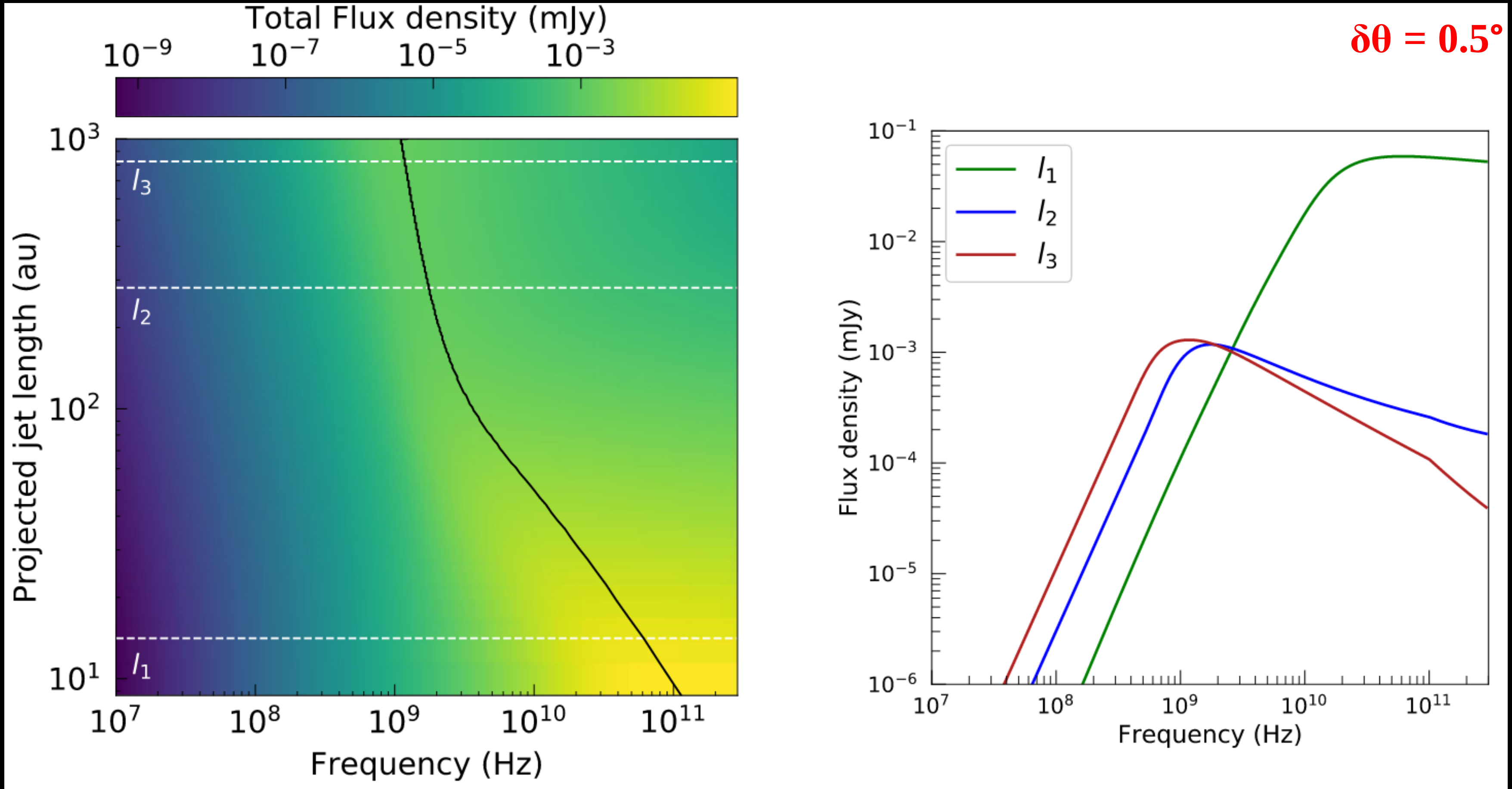

- $r0 = 3000$ au
- $\theta 0 = 30°$
- $\eta e = 10^{-5}$
- $p = 2.3$
- $B = 0.3$ mG
- $n0 = 500\ cm^{-3}$
- $x0 = 0.2$
- $qx = -0.5$
- $qx = -1$

Flux variation across jet length

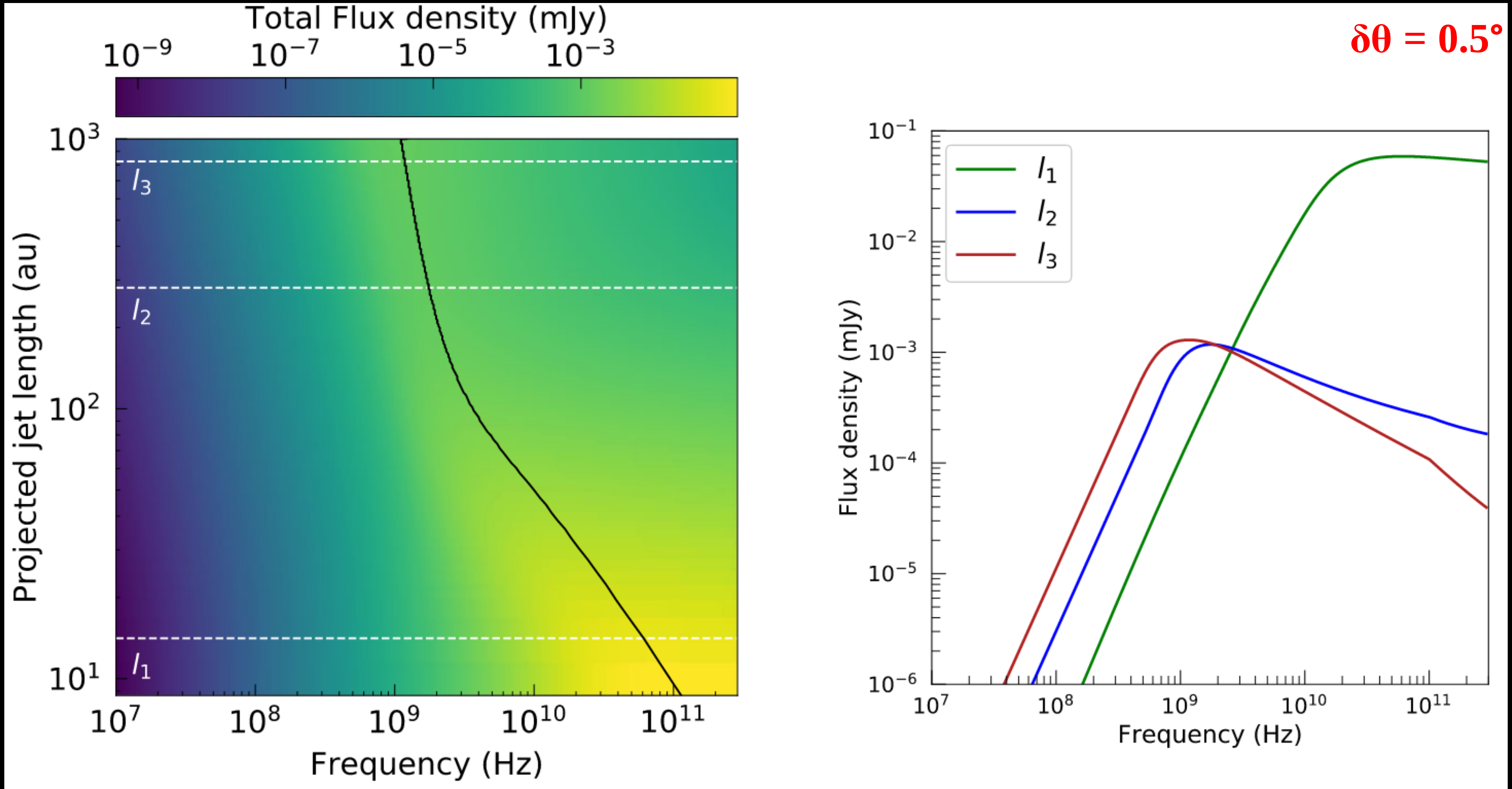

$j_{\nu,syn}, \alpha_{\nu,syn}, \tau_{\nu,syn} \propto n\ x$

$j_{\nu,ff}, \alpha_{\nu,ff}, \tau_{\nu,ff} \propto n^2\ x^2$

Jet radio spectrum

- To study the **transition from free-free to synchrotron** dominated spectrum
- Case of a jet with a combination of both free-free and synchrotron emission
- η_e: Fraction of relativistic electrons capable of emitting synchrotron
- η_e is varied to regulate the contribution of synchrotron on the overall jet spectrum

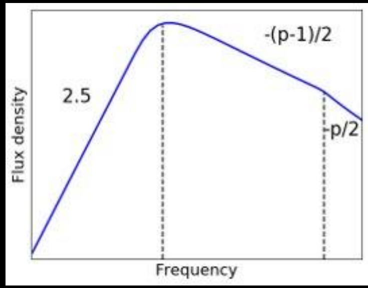

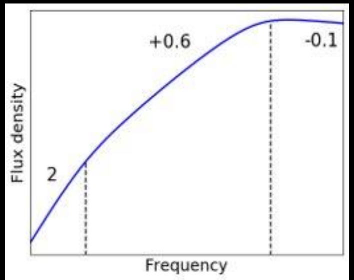

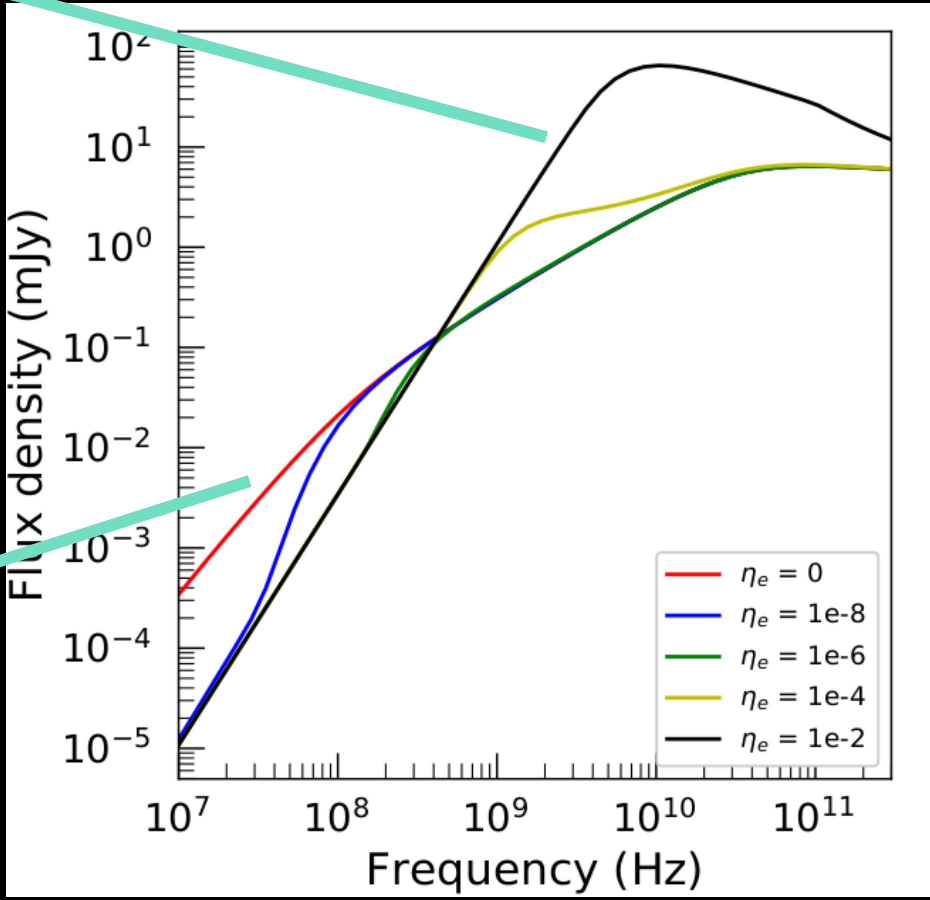

Application of the model

Comparison of model with Observations

Determination of knot parameters from observations

$$\text{size} = \theta_{maj}$$

$$r_0 = \text{radial distance of the knot center} - \frac{\text{size}}{2}$$

$$\theta_0 = 2\tan^{-1}\left(\frac{\theta_{min}}{2r_0}\right)$$

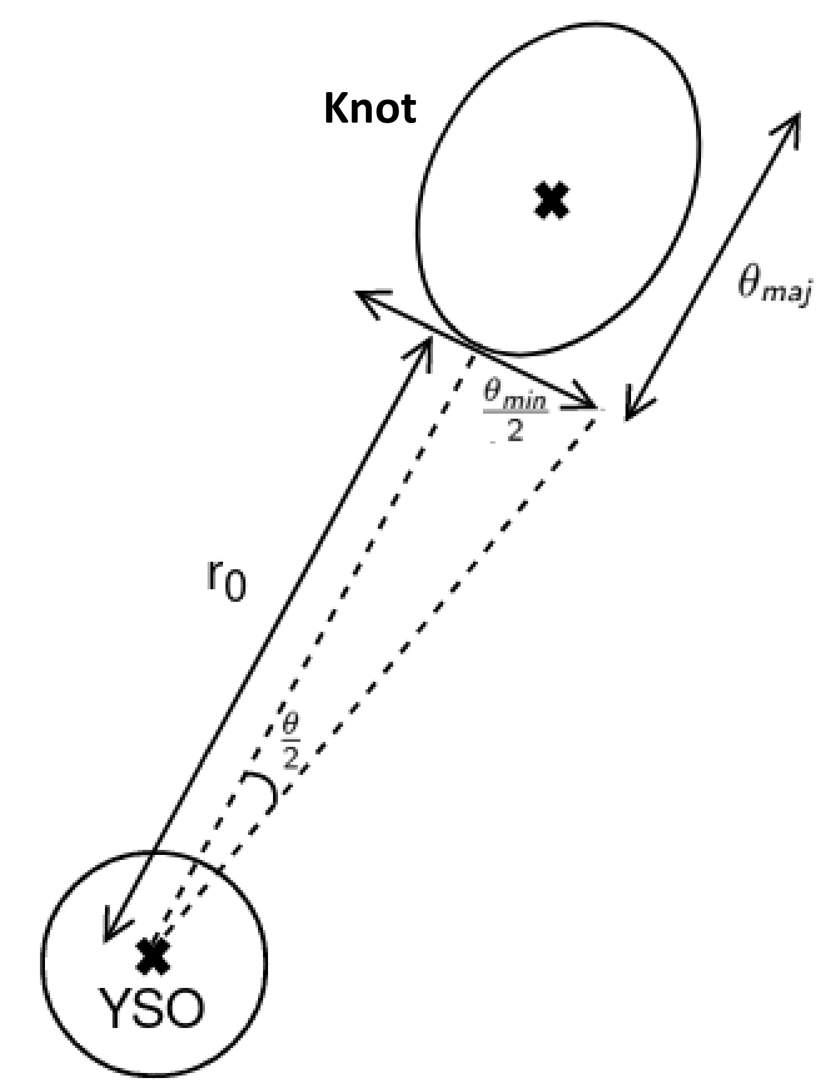

Comparison of model with Observations

Assumed knot parameters based on knowledge from observations and models:

- **T = 10^4 K**
- **ε = 2/3 and 3/4 (Reynolds 1986)**

$$w(y) = w_0 \left(\frac{r_a}{r_0}\right)^{\epsilon} = w_0 \left(\frac{y}{y_0}\right)^{\epsilon}$$

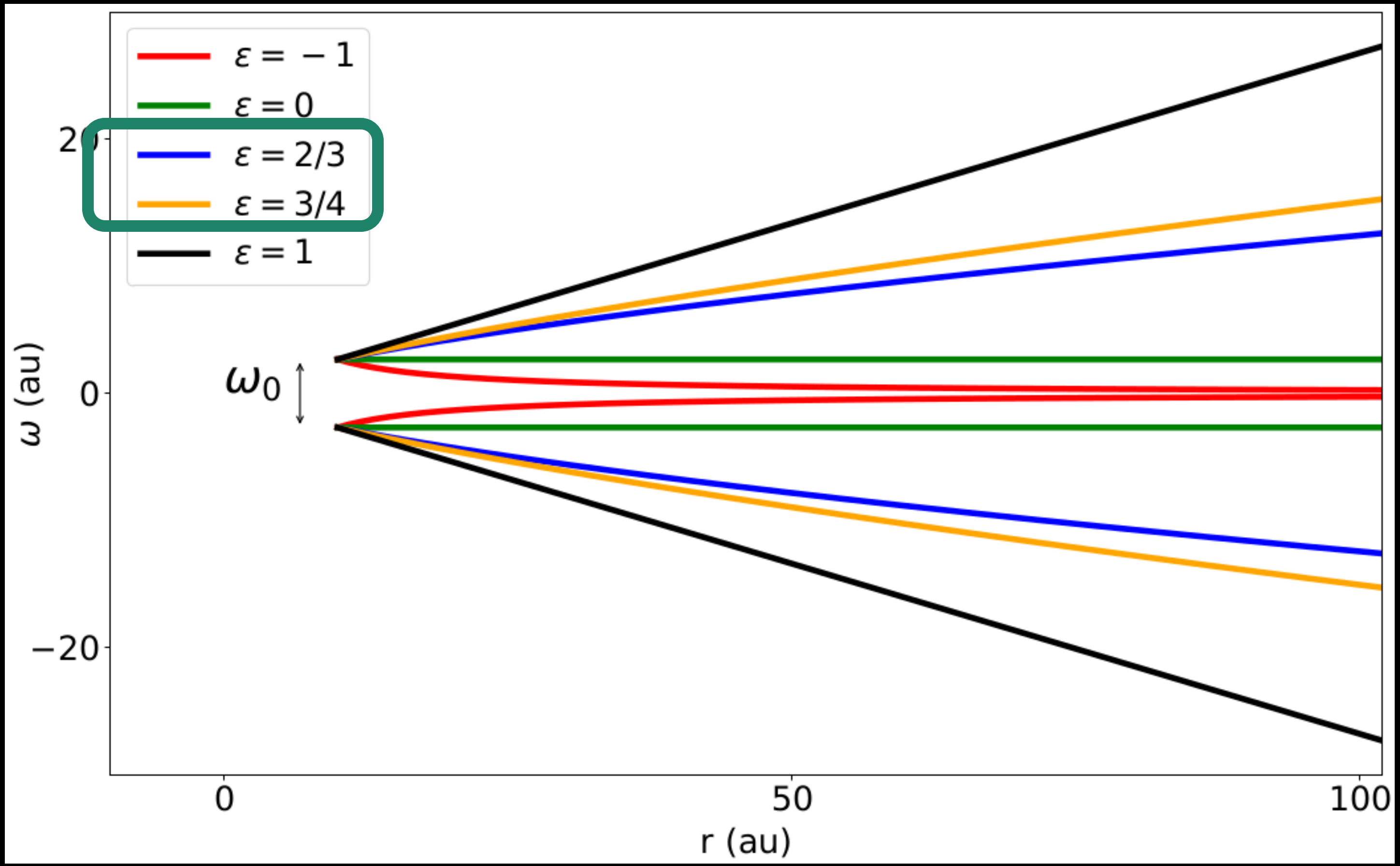

Best-fit model: Model grids generated

- q_n, q_x, q_x', $\delta\theta$, p, η_e: Physical parameters that are difficult to be constrained by observations.
- For few jets, n_0 measurement is not available: $n_0 * x_0$

Parameters	Range Explored and Grid spacing
Number density at jet base (n_0 [cm^{-3}])	10^2 to 10^6 by a factor of 10
Power-law index of radial number density variation (q_n)	-4 to -1 in steps of 0.5
Power-law index of radial ionization fraction variation (q_x)	-5 to 0 in steps of 0.5
Power-law index of lateral ionization fraction variation (q'_x)	-5 to 0 in steps of 0.5
Angular thickness of shocked region ($\delta\theta$ [°])	0.01 to 0.5 in steps of 0.1
Power-law index of non-thermal electron population (p)	1.7 to 2.6 in steps of 0.1
Fraction of relativistic electrons (η_e^{rel})	10^{-7} to 10^{-4} by a factor of 10

Case I: HH80-81

- **High mass protostar: 11-15 $M_\odot$**
- **Distance: 1.4 kpc**

Fernandez-Lopez et al. 2011, Anez-Lopez et al. 2020

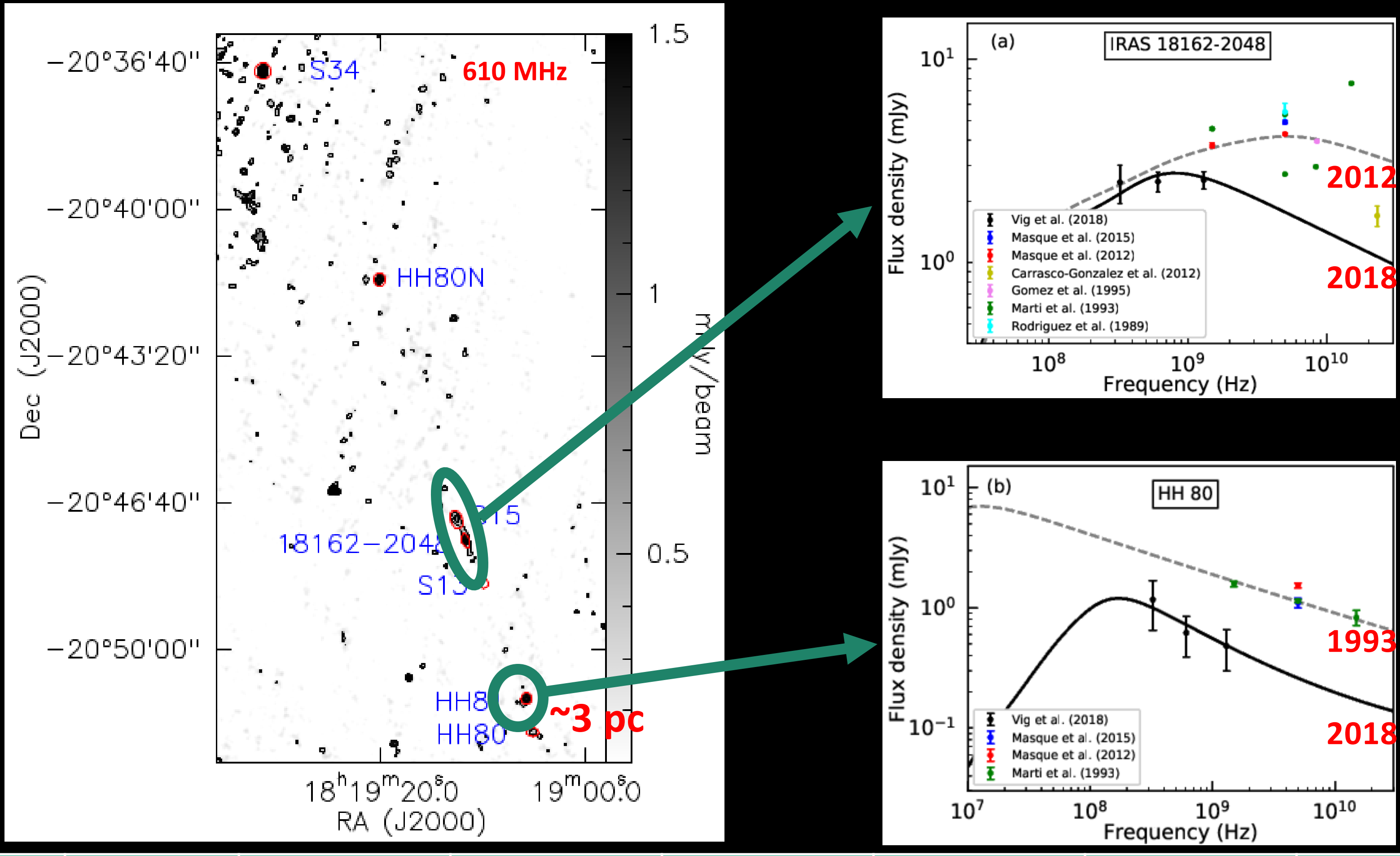

Vig et al. 2018

Model	ε	$n_0{*}x_0$	q_n	q_x	$q_{x'}$	δθ	p	η_e	χ^2
18162/2016	2/3	4.5×10^4	-1	-0.2	0.0	0.10	1.7	1×10^{-4}	0.87
18162/2009	2/3	3×10^5	-2	-0.5	0.0	0.10	1.7	1×10^{-4}	0.60
HH80/2016	2/3	200	-2	-2.5	-3.5	0.01	2.3	1×10^{-6}	0.30
HH80/1989	2/3	200	-3	-0.2	-3.0	0.01	1.7	1×10^{-6}	1.07

Case II: Serpens Triple radio source

- Intermediate mass protostar: 3 $M_\odot$
- Distance: 436 pc

Hull et al. 2016, Ortiz-Leon et al. 2017

Curiel et al. 1993

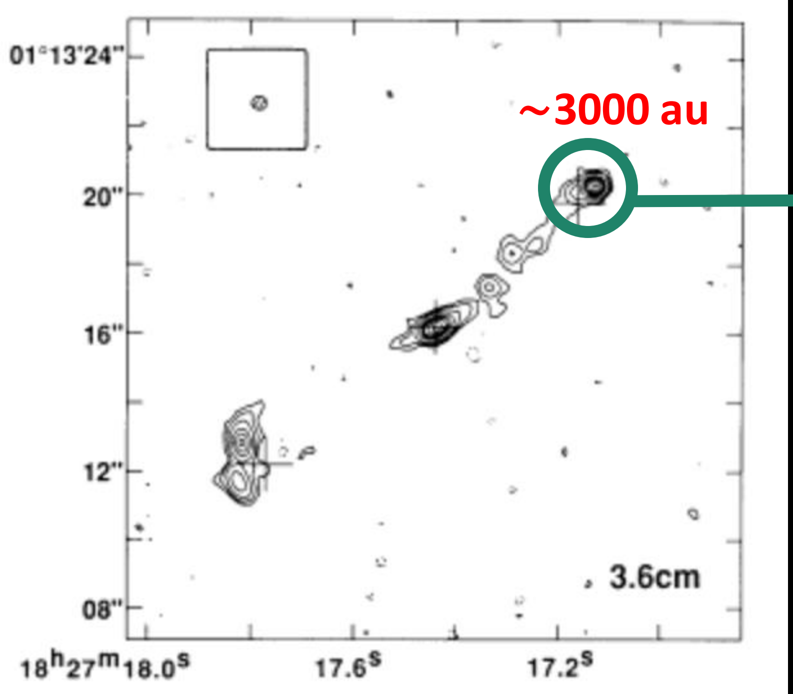

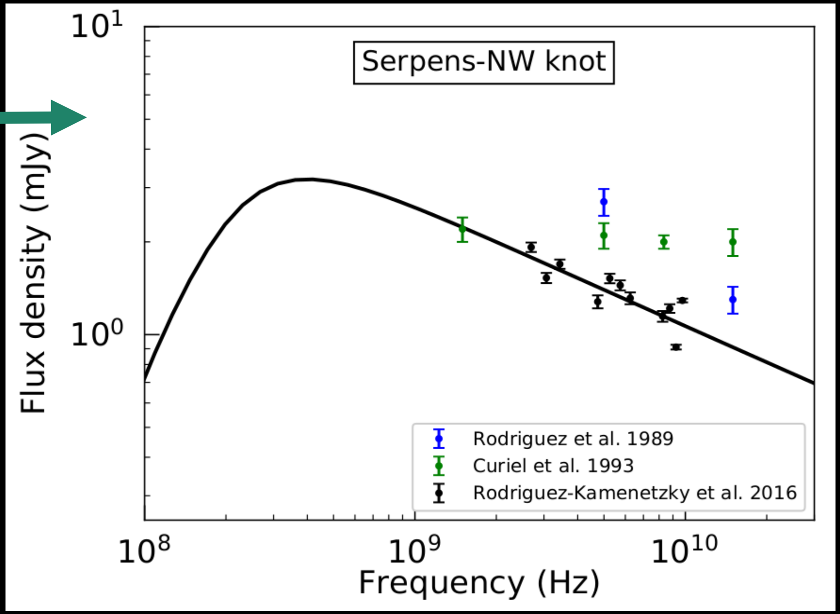

ε	$n_0 * x_0$	q_n	q_x	$q_{x'}$	δθ	p	η_e	χ2
2/3	1.2×10^4	-1	-1	0	0.5	1.8	1×10^{-6}	319.3

Case III: DG Tau A

- Low mass protostar: 0.67 $M_{\odot}$
- Distance: 120 pc

Lynch et al. 2013, Bailer-Jones et al. 2018

Feeney Johansson et al. 2019

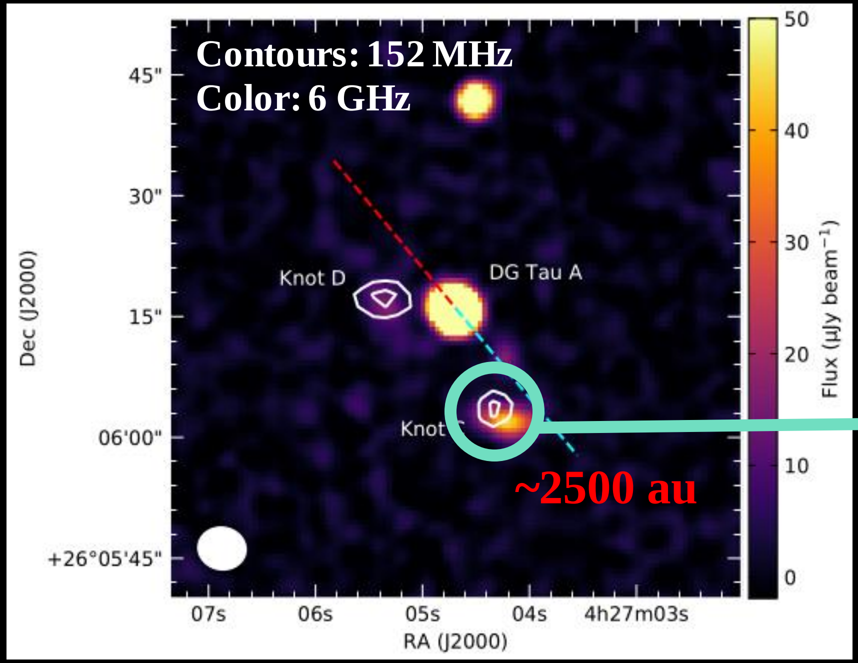

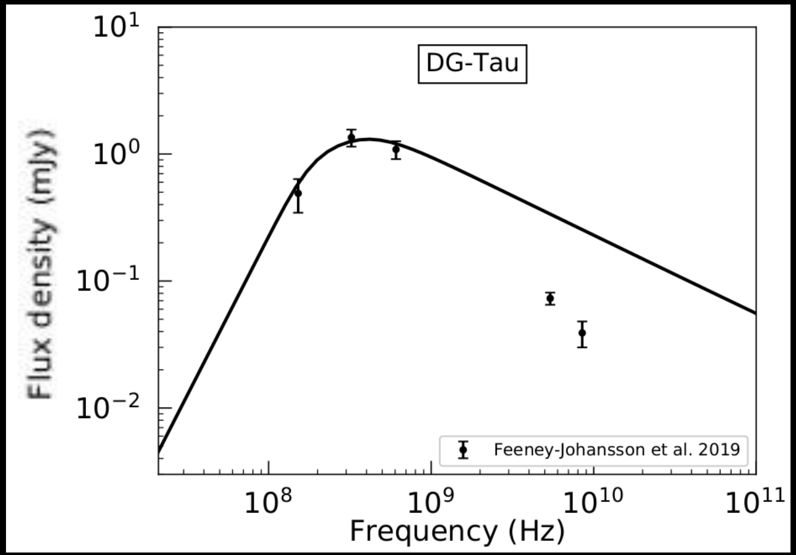

ε	$n_0 * x_0$	q_n	q_x	$q_{x'}$	δθ	p	η_e	χ2
3/4	500	-3	-1	0	0.2	2.25	1×10^{-5}	47.8

Summary

- Features of our new model developed for protostellar jets:
  - Thermal free-free + non-thermal synchrotron emission
  - Lateral variation in ionization fraction
  - Generalized geometry and optical depth calculations

- Model can be employed to estimate physical parameters that are difficult to be constrained from observations.
- Model has been applied to few protostellar jets (HH80-81, Serpens triple radio source and DG-Tau) to estimate jet parameters that were unknown due to observational limitations.
- The estimated parameters (q_n,p,η_e) are reasonable and consistent with expected values from jet shock models etc.